# FEASIBILITY STUDY OF THE FRICTION SURFACING PROCESS

F. Swinnen[1], K. Faes[2] and W. De Waele[3]

[1] Ghent University, Belgium
[2] Belgian Welding Institute (BWI), Belgium
[3] Ghent University, Laboratory Soete, Belgium

**Abstract:** Friction surfacing is a solid state cladding process based on the plastic deformation of a translating and rotating metallic consumable rod pressed against a stationary substrate. It is mostly used on mild and stainless steel and on aluminium. Thanks to the solid state nature of the process, it allows to join dissimilar metal combinations, e.g. aluminium to steel or to ceramics or several combinations of non-ferrous metals. Moreover, a continuous and fine-grained deposition is formed. Most research has been focussed on the feasibility of certain material combinations and on correlating the deposited layer quality to input parameters. In this work, a methodical approach to evaluate clad layers and to assess their properties is discussed. This approach consists of a visual assessment, a macrographic examination and a performance analysis and has shown to be apt to compare the clad layer quality.

**Keywords:** friction surfacing; aluminium; visual assessment; macrographic examination; performance analysis

## 1 INTRODUCTION

To clad metals, fusion welding techniques are amongst the most frequently used. Nevertheless, these processes have their shortcomings; they are prone to a variety of metallurgical problems such as cast microstructures, inhomogeneities, solidification cracking, the presence of residual stresses and the formation of brittle intermetallic phases [1]. To overcome these problems, alternative processing technologies based on friction have been developed [1,2].

Friction surfacing is one of these technologies. It is a solid state deposition process based on the plastic deformation of a translating and rotating metallic consumable rod pressed against a stationary substrate, cf. Fig. 1. Main applications include repair of worn or damaged surfaces through building up or crack sealing. It has also been applied to enhance surface properties at specific areas in the manufacturing of parts and tools [2]. Moreover, it has gained renewed attention due to its potential in the field of additive manufacturing [3].

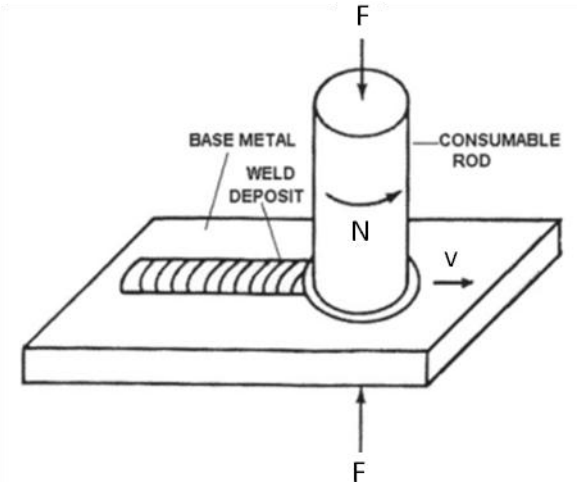


Fig. 1: Friction surfacing schematic, adapted from [4].

Nowadays, research is mainly focussed on the feasibility of material combinations and on correlating the surface layer quality to process parameters [2]. To a lesser extent, applications and technological innovations are examined [5]. In this work, the authors propose a methodical approach to evaluate clad layers and to assess their properties. For this purpose, aluminium substrates and consumable rods have been used.

## 2 WORKING PRINCIPLE OF FRICTION SURFACING

The process consists of four main stages. A consumable rod is rotated (stage 1) and pushed against the substrate (stage 2). The rotating rod causes a plane of shear at the contact surface where frictional heat is created. This leads to a prominent temperature increase in the lower part of the rod, creating a viscoplastic boundary layer at its tip. The substrate, on the other hand, maintains a lower temperature due to its relatively large dimensions, facilitating a heat sink. The combination of pressure and temperature then leads to an interdiffusion process resulting in a strong bond between the rod tip and the substrate. Thanks to the viscoplastic boundary layer at the extremity of the rod, the metal detaches from it and is retained by the substrate (stage 3). Heat conduction in the substrate allows for the bonded metal to consolidate. In this way, the viscoplastic shearing interface moves away from the substrate surface, increasing the thickness of the layer left behind. After this dwelling phase, the rod starts travelling in the transverse direction (stage 4) following any desired, pre-programmed path [2,4].

Depending on the application, two operations can be performed using friction surfacing: depositing a single layer or several layers onto each other. In terms of single-layered deposits, it is possible to achieve a great variety of positions and designs thanks to the absence of fusion and the fast cooling rates [2]. Moreover, it is possible to cover an entire area by depositing several of these layers next to each other. The second approach consists of vertically building up overlapping layers, the so-called multi-layer depositions. Layers can be put on top of each other without any intermediate milling, but degreasing is necessary for sound depositions [2].

Similar as for other solid state joining processes, the main advantages of friction surfacing are a small and thin heat affected zone in the substrate, the possibility to join dissimilar materials, only a limited presence of residual stresses and a low required heat input. Apart from that, it guarantees a continuous and fine-grained coating layer and it is usable for materials that are not easily weldable. The process has some drawbacks as well. Due to the formation of a revolving flash around the rotating consumable rod, not all material is transferred to the substrate. Additionally, there is no bonding at the coating edges. Apart from these limitations regarding material efficiency, another disadvantage is that there are only three controllable process parameters: rotational speed, transverse speed and axial force [2].

Since there are many applications of mild and stainless steel and aluminium, most early research on friction surfacing focussed on these particular materials [6–8]. However, this does not mean that friction surfacing is limited to these materials. Even though they have often proven to pose additional challenges, also other non-ferrous metals have been joined successfully to each other and to ceramics [9–11].

## 3 FRICTION SURFACING TRIALS

### 3.1 Friction welding equipment

The machine used for the friction surfacing experiments is an adapted version of the friction welding machine of the Belgian Welding Institute, cf. Fig. 2, [12–14].

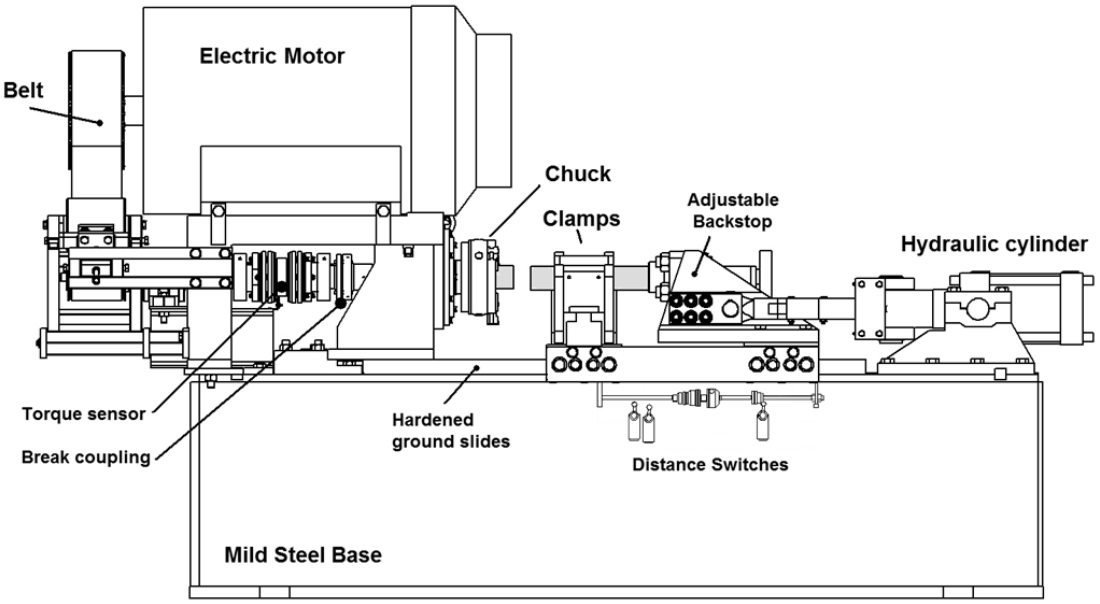


Fig. 2: Overview of the basic components of the friction welding machine [12].

The friction welding machine makes use of clamps to hold the parts to be welded. For friction surfacing, a transverse sliding mechanism, shown in Fig. 3, has been designed to replace the clamps in Fig. 2.

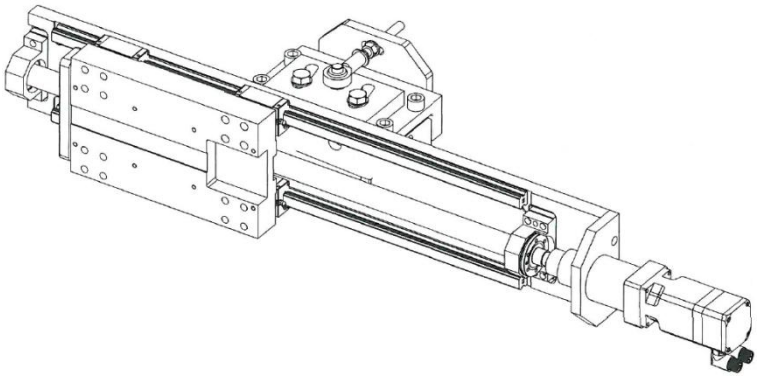

Fig. 3: Transverse sliding mechanism.

This system is based on an anvil (holding the plate) connected to two rails through four runners. On one side, a nut enables this assembly to shift along a motor driven ball screw.

Furthermore, to compensate for the induced transverse forces that are not present during friction welding, a support system for the chuck has been installed.

### 3.2 Materials and methods

In this work, deposition of aluminium alloy EN AW-6063-T6 onto aluminium EN-AW-5083-H11 has been investigated. Consumable rods with a diameter of 30 mm and substrate plates with a thickness of 6 mm have been used. All three input parameters (axial force F, rotational speed N and transverse speed v; cf. Fig. 1) have been varied. The axial force (controlled using a proportional valve in the hydraulic circuit) was set at two levels: approx. 10 and 12 kN. The applied rotational speeds were chosen as 800, 1000 and 1200 rpm and the transverse speeds as 3,5; 5,3 and 7,2 mm/s.

During the course of the experiments, the following variables were recorded: the rotational speed of the rod, the axial position of the substrate (which is approaching the chuck), the transverse position of the substrate and the axial force. An example of a typical course of these variables is shown below.

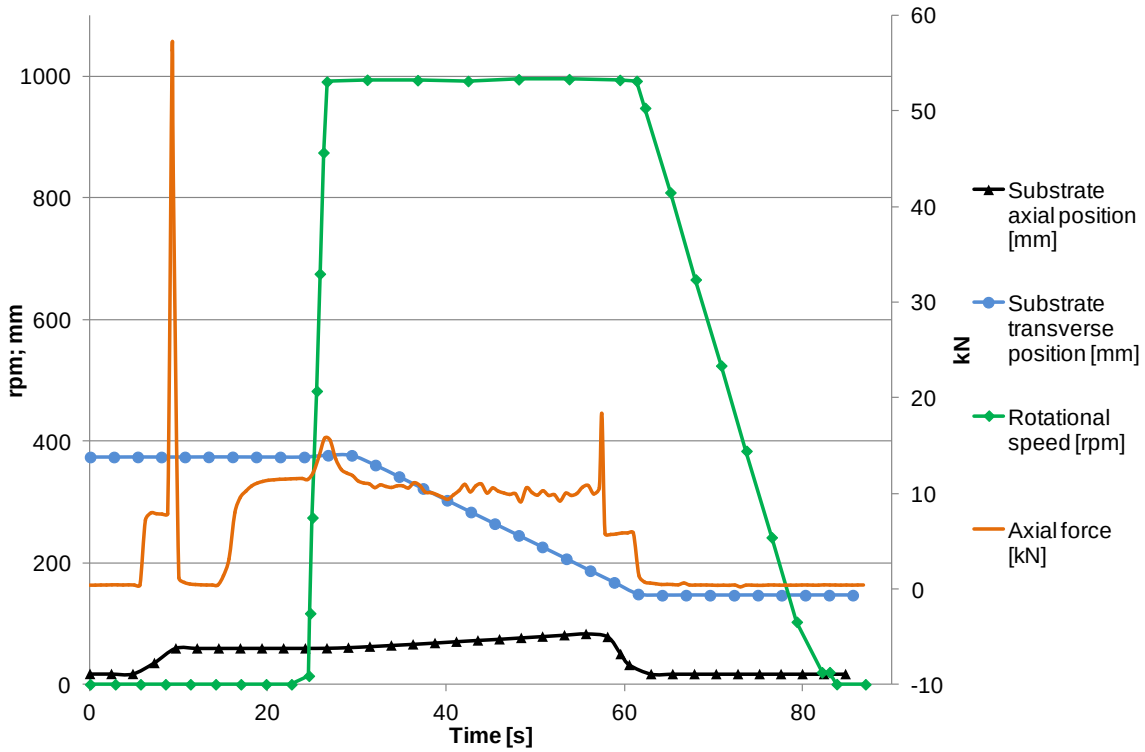


Fig. 4: Typical course of the measured variables.

### 3.3 Quality evaluation

In order to assess the quality of the deposited layers in a consistent way, an evaluation framework based on mechanical testing, visual assessment, metallographic examination and performance analyses is under development. This paper focuses on the visual assessment, metallographic examination and performance analysis.

#### *3.3.1 Visual assessment*

For applications involving stacked or adjacent layers, it is important for these layers to have a uniform thickness and width respectively. Variations in roughness are also considered important since it might have an impact on the required post-processing (milling etc.).

In order to categorise the quality of the coatings based on the uniformity of thickness, width and roughness, a scoring system based on visual inspection is suggested. A score out of three is given to each of these characteristics. Typical visual aspects related to a score of either 1, 2 or 3 for the thickness, width and roughness are depicted in Fig. 5, Fig. 6 and Fig. 7, respectively.

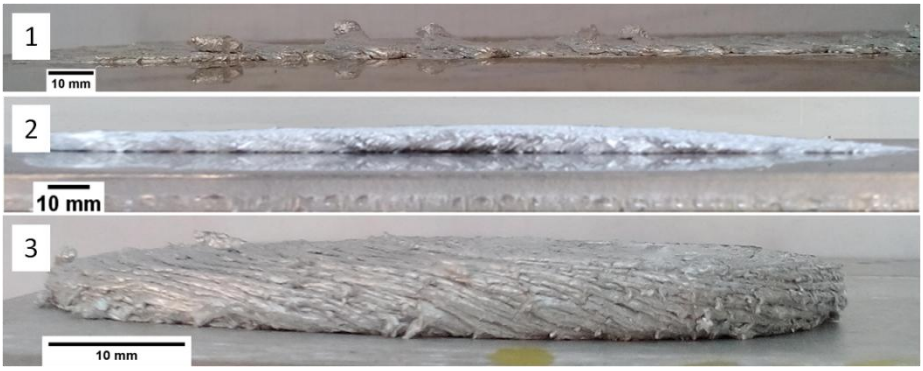


Fig. 5: Typical score values for the thickness.

The upper coating in the figure above shows irregular flash formation and several sudden changes in thickness and is therefore attributed a score of 1. The middle coating is smooth, but does not have a constant thickness. Hence, it was given a score of 2. The lower coating has a score of 3 because it shows a constant thickness (apart from the transitional zone on the left hand side).


Fig. 6: Typical score values for the width.

The coatings shown in Fig. 6 demonstrate an increasing degree of width uniformity. The upper coating shows large differences in width depending on the transverse position. The width around the narrowest sections is not more than a fraction of the width around the widest sections, resulting in a score of 1 for this

coating. The middle one also shows differences, but only to a limited extent. Thus, a score of 2 is appropriate. The lower one, finally, demonstrates an almost constant width and is therefore granted a score of 3.

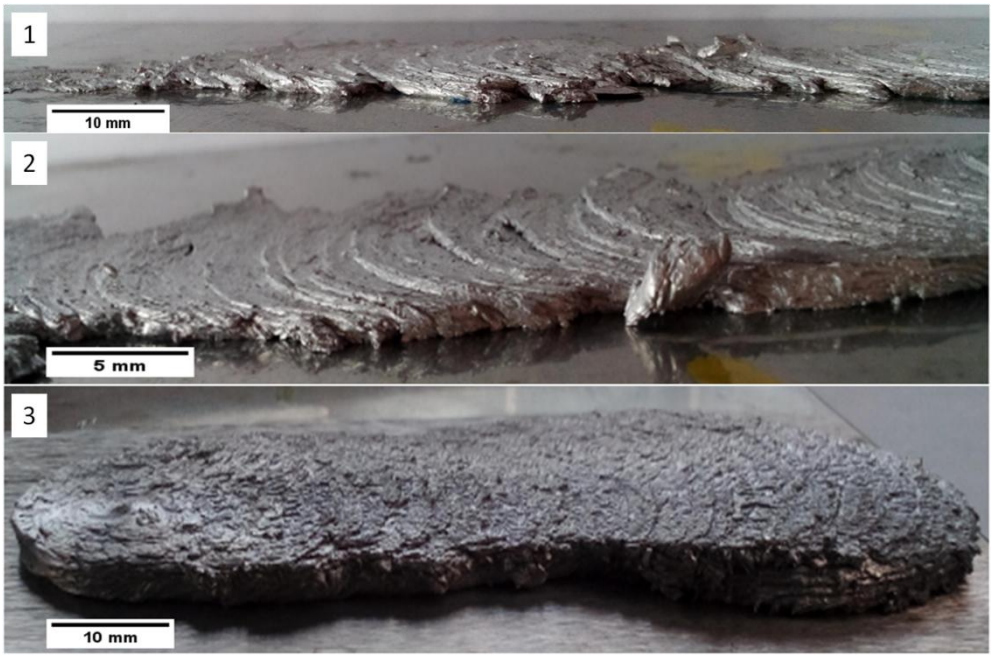


Fig. 7: Typical score values for the roughness.

Fig. 7 displays a decreasing degree of roughness. As can be seen, the coating with a score of 1 is very irregular. The elliptically shaped waves of subsequently released material are not always visible. The middle coating does show those ellipses clearly, but the distance between them varies. This is in contrast with the lower coating, which has a regular and smooth surface.

Depending on the contemplated application, a weight factor can be attributed to the scores in order to combine them into a final visual score which can be determined as the weighted average. Some values suggested by the authors (mainly based on the importance of dimensions and necessity of post-processing) can be found in Table 1.

Table 1: Recommended values for normalised weights for calculating the final visual score.

| | **Thickness** | **Width** | **Roughness** |
|---|---|---|---|
| Adjacent layers | 0,3 | 0,5 | 0,2 |
| Built-up layers | 0,4 | 0,3 | 0,3 |
| Filling of a groove | 0,2 | 0,6 | 0,2 |

### *3.3.2 Macrographic examination*

Apart from evaluating the consistency of the dimensions along the direction of transverse movement, the dimensions are also evaluated at a representative point along the transverse direction.

These dimensions can be measured using a macrograph of a cross-section. An example (generated using an Olympus MX51) is shown in Fig. 8. Due to dimensional restrictions, it was necessary to cut the specimens by grinding. This has been taken into account when determining the width. The grinding disk has a thickness of 1,5 mm, which was added to the measured width.

Measuring the thickness, on the other hand, poses another challenge. As can be seen on the figure below, the thickness varies across the width. In order to compare the thickness of different coatings in a consistent way, it has been chosen to measure it at the ground edge. For some depositions, including the one below, there is evidence of plastic deformation of the substrate. For the sake of uniformity, the thickness was measured from the original substrate boundary.


Fig. 8: Typical macrograph of a cross-section.

Another characteristic is porosity. This can be quantified performing an analysis using scientific image processing software.

Since there is typically no bonding at the coating edges, the width as measured on this kind of image is larger than the usable width. At higher magnifications, however, it is also possible to determine the bonded width.

Finally, through etching of the specimen (cf. Fig. 9) it is possible to gain insight into material flow patterns, dilution and the size of the heat affected zone.


Fig. 9: Typical macrograph of an etched cross-section.

### *3.3.3 Performance analysis*

Based on the dimensions discussed in paragraph 3.3.2, it is possible to compare the bonded to the deposited width. The bonding efficiency can be calculated as

$$\eta_{bonding} = \frac{bonded\ width}{deposited\ width} \tag{1}$$

Another performance indicator is related to material efficiency. Due to flash generation at the rod tip, not all material is transferred to the substrate. By mass measurements of the rod and the substrate before and after deposition, it is possible to determine how much material was effectively deposited. The volume of the material that could have been deposited under the most optimal conditions (no flash generation), can be calculated by measuring the shortening of the rod. Calculating the ratio of these two values yields the deposition efficiency:

$$\eta_{deposition} = \frac{mass\ deposited}{\rho\ \Delta l\ \pi\ D^2/4} \tag{2}$$

In this equation ρ is the density, Δl the shortening and D the diameter of the rod.

Combining these two efficiencies leads to the global efficiency:

$$\eta = \eta_{bonding} \cdot \eta_{deposition} \tag{3}$$

## 3.4 Results

After visual inspection of the depositions, it has been noticed that most of the discussed combinations lead to smooth and consistent depositions with visual scores (omitting weight factors) ranging from 2,33 to 3.

The influence of the input variables on the dimensions (obtained using macrographic examination) is plotted below. From these graphs, it can be seen that both thickness and width tend to increase at higher

forces. Most likely, the reason for this observation is the fact that the head generation at the rod tip is proportional to the axial force and rotational speed. Thus, for a constant rotational speed, higher forces correspond to a higher increase of temperature in the rod tip. This in turn leads to a larger portion of the rod in a viscoplastic state and therefore more deposited material. This is not the case for all measurements, however, proving the relevance of the influence of the other parameters as well.

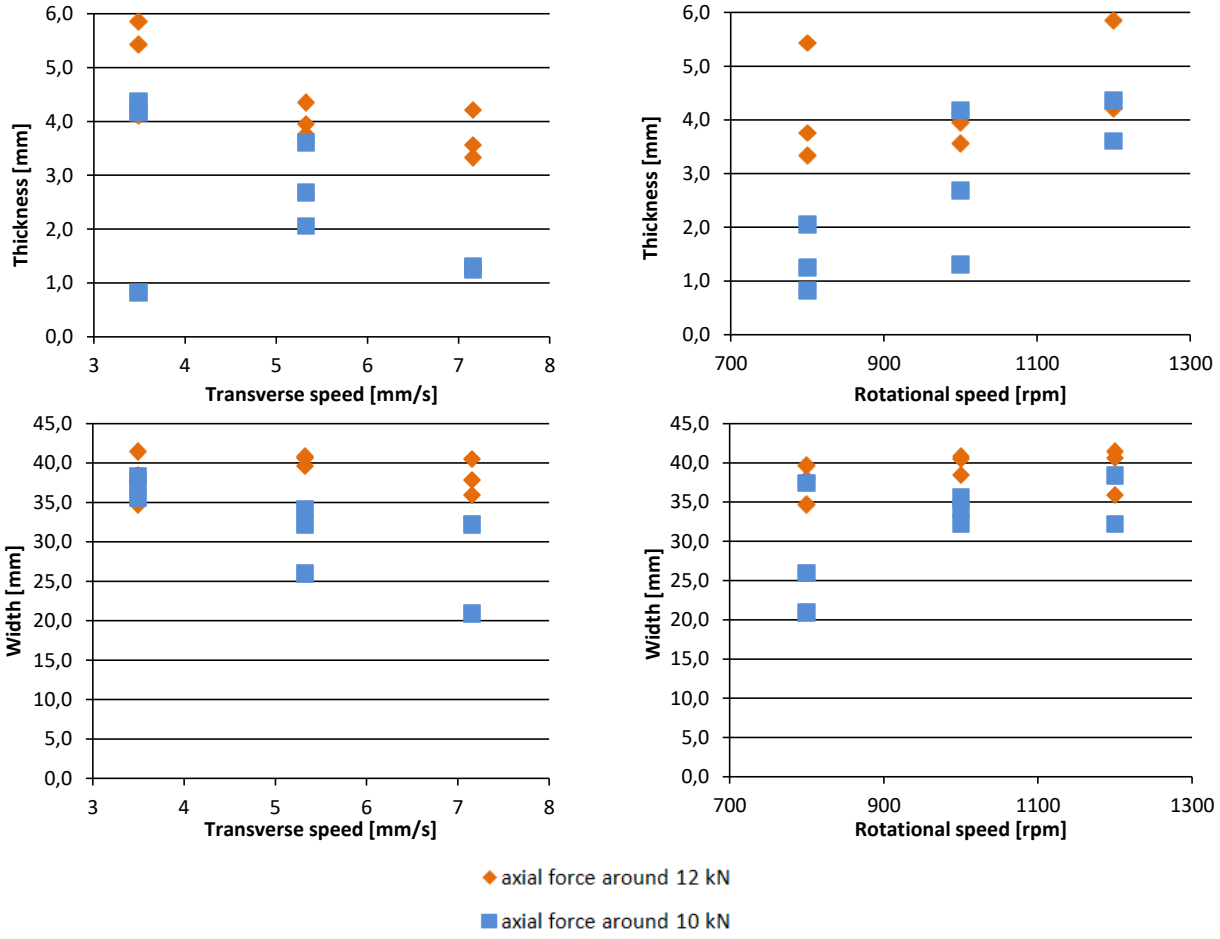


Fig. 10: Clad layer dimensions as a function of the input variables.

Fig. 10 also shows that, in general, increasing rotational speed corresponds to increasing thickness and width. Like axial force, rotational speed has an influence on temperature increase and thus also on material deposition. Transverse speed, on the contrary, has the opposite effect. When the rod moves faster with respect to the substrate, less time is available for the material to be deposited at a certain location, resulting in thinner, but longer coatings.

The influence of the input variables on bonding and deposition efficiency is unclear. Fig. 11 shows that the effect of the axial force is manifested mainly in efficiency range. The average bonding efficiency equals 82 % at both force settings. The average deposition efficiency, on the other hand, decreases from 66 % to 60 % at higher forces. Opposed to this slight difference in average efficiency, it is clear that the efficiency range is remarkably affected. At higher forces, it decreases for any kind of efficiency.

Since the average efficiency tends to be in the upper half of the range, most of the probed sets of parameters show good results. Combinations of high transverse and rotational speeds tend to result in low bonding efficiencies. This is probably due to the formation of more irregular coating edges and the lack of time for these to bond to the substrate. Low deposition efficiencies occur mainly in case of low rotational speed. From this, it can be concluded that – for both levels of axial force – intermediate rotational and transverse speeds have the tendency to lead to efficient depositions.

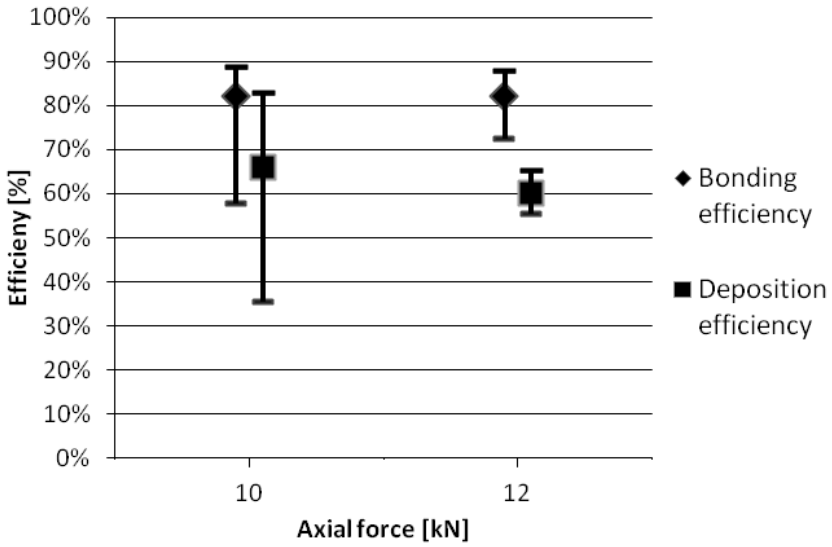


Fig. 11: Effect of axial force on efficiency.

## 4 CONCLUSIONS

This study on friction surfacing of aluminium has lead to the following conclusions:

- The proposed testing procedure has shown to be applicable and apt to compare the quality of different coatings. Further development with the introduction of additional output variables and a way to combine them into a final variable is however necessary.
- The coating thickness and width tend to increase for an increasing axial force and rotational speed and decrease for an increasing transverse speed. Nevertheless, the combined effect of these input variables remains unclear and needs further investigation.
- The average values of the bonding and deposition efficiency only vary slightly with the axial force. Their ranges have been found to decrease with increasing force. For both levels, intermediate rotational and transverse speeds lead to the best results.

## 5 NOMENCLATURE

| | | |
|---|---|---|
| F | axial force | kN |
| N | rotational speed | rpm |
| v | transverse speed | mm/s |
| ρ | rod material density | g/mm³ |
| $\Delta l$ | shortening of the rod | mm |
| D | diameter of the rod | mm |
| $\eta_{bonding}$ | bonding efficiency | - |
| $\eta_{deposition}$ | deposition efficiency | - |
| η | global efficiency | - |

## 6 ACKNOWLEDGEMENTS

The authors would like to acknowledge the support of Philip De Baere and Sam Demeester (BWI) in assembling the installation and preparing the experiments and the support of Michel De Waele and Gert Oost (BWI) in processing specimens.

## 7 REFERENCES

[1] Dilip, J. J. S., Ram, Gdj., and Stucker, B. E., 2012, 'Additive Manufacturing with Friction Welding and Friction Deposition Processes', Int. J. Rapid Manuf., **3**(1), pp. 56–69.

[2] Gandra, J., Krohn, H., Miranda, R. M., Vilaça, P., Quintino, L., and Dos Santos, J. F., 2014, 'Friction Surfacing - A Review', J. Mater. Process. Technol., **214**(5), pp. 1062–1093.

[3] Dilip, J. J. S., Babu, S., Rajan, S. V., Rafi, K. H., Ram, G. D. J., and Stucker, B. E., 2013, 'Use of Friction Surfacing for Additive Manufacturing', Mater. Manuf. Process., **28**(2), pp. 189–194.

[4] Chattopadhyay, R., 2004, 'Friction Weld Surfacing', *Advance Thermally Assisted Surface Engineering Processes*, Springer, pp. 219–227.

[5] Li, M., 2015, 'Development and Prospect of Friction Surfacing Technology', (Kam), pp. 244–246.

[6] Thomas, W. M., Nicholas, E. D., and Dunkerton, S. B., 1984, *Feasibility Studies into Surfacing by Friction Welding*, Cambridge.

[7] Thomas, W. M., 1986, *The Deposition of Hardfacing, Corrosion Resistant and Non-Ferrous Material by Friction Surfacing*.

[8] Thomas, W. M., 1986, *Process Characteristics When Friction Surfacing Mild Steel with Austenitic Stainless Steel*.

[9] Dilip, J. J. S., and Janaki Ram, G. D., 2013, 'Microstructure Evolution in Aluminum Alloy AA 2014 during Multi-Layer Friction Deposition', Mater. Charact., **86**, pp. 146–151.

[10] Rao, K. P., Sankar, A., Rafi, H. K., Ram, G. D. J., and Reddy, G. M., 2012, 'Friction Surfacing on Nonferrous Substrates: A Feasibility Study', Int. J. Adv. Manuf. Technol., pp. 1–8.

[11] Mirlashari, A., 2010, 'Micro-Friction Surfacing on Ceramics', TWI Bull., (March-April).

[12] Rombaut, P., 2010, 'Joining of Dissimilar Materials through Rotary Friction Welding', Ghent University.

[13] Rombaut, P., De Waele, W., and Faes, K., 2011, 'Friction Welding of Steel to Ceramic', Sustain. Constr. Des., **2**(3), pp. 448–457.

[14] Bonte, D., Derynck, B., De Baets, P., De Waele, W., and Faes, K., 2010, 'Friction Welding of Ceramics to Metals', Sustain. Constr. Des., **1**(1), p. 14.